

# GK Boo and AE For: Two low-mass eclipsing binaries with dwarf companions<sup>★</sup>

P. Zasche<sup>1</sup>, P. Svoboda<sup>2</sup>, and R. Uhlář<sup>3</sup>

<sup>1</sup> Astronomical Institute, Faculty of Mathematics and Physics, Charles University Prague, CZ-180 00 Praha 8, V Holešovičkách 2, Czech Republic, e-mail: zasche@sirrah.troja.mff.cuni.cz

<sup>2</sup> Private observatory, Výпустky 5, Brno, CZ-614 00 Czech Republic

<sup>3</sup> Private Observatory, Pohoží 71, 25401 Jílové u Prahy, Czech Republic

November 13, 2018

## ABSTRACT

**Context.** A study of late-type low-mass eclipsing binaries provides us with important information about the most common stars in the Universe.

**Aims.** We obtain the first light curves and perform period analyses of two neglected eclipsing binaries GK Boo and AE For to reveal their basic physical properties.

**Methods.** We performed both a period analysis of the times of the minima and a *BVR* light curve analysis. Many new times of minima for both the systems were derived and collected from the data obtained by automatic and robotic telescopes. This allowed us to study the long-term period changes in these systems for the first time. From the light curve analysis, we derived the first rough estimates of the physical properties of these systems.

**Results.** We find that the analyzed systems are somewhat similar to each other. Both contain low-mass components of similar types, both are close to the Sun, both have short orbital period, and both contain another low-mass companions on longer orbits of a few years. In the case of GK Boo, both components are probably of K3 spectral type, while the distant companion is probably a late M star. The light curve of GK Boo is asymmetric, which probably causes the shift in the secondary minima in the *O–C* diagram. System AE For comprises two K7 stars, and the third body is a possible brown dwarf with a minimal mass of only about  $47 M_{Jup}$ .

**Conclusions.** We succeed in completing period and light curve analyses of both systems, although a more detailed spectroscopic analysis is needed to confirm the physical parameters of the components to a higher accuracy.

**Key words.** binaries: eclipsing – stars: fundamental parameters – stars: individual: GK Boo, AE For

## 1. Introduction

Low-mass stars are the most common stars in our Galaxy (e.g. Kroupa 2002). However, owing to their low luminosity, only these close to the Sun have been studied in detail and many of them have never been analyzed. Hence, we focused on two rather neglected low-mass eclipsing binary systems: GK Boo and AE For. Their light curves as well as their period modulation had never been studied. Some studies indicate that most late-type stars are single (e.g. Lada 2006), but the number of papers studying the multiplicity of the late-type systems is still rather limited. Therefore, the incidence of multiples in late-type stars remains unexplored.

The study of eclipsing binaries provide us with important information about the physical properties of both of their components – their radii, masses, and evolutionary status. However, when considering only with the light curve, several assumptions have to be made. For the analysis presented in this paper we also used the photometric data obtained by automatic and robotic telescopes (such as ASAS, Pi of the sky, and SWASP). Thanks to these huge databases of observations, the long-term evolution of these systems can be studied for the first time.

## 2. GK Boo

### 2.1. Introduction

The system GK Boo (= BD+37 2556,  $V_{max} = 10.86$  mag) is an Algol-type eclipsing binary with an orbital period of about 0.48 day. It is also a primary component of a visual double designated WDS J14384+3632 in the Washington Double Star Catalog (WDS<sup>1</sup>, Mason et al. 2001). The secondary component of this double star is about  $14''$  distant, and is probably gravitationally bound to GK Boo itself. It is about 0.4 mag fainter, but since its discovery in 1933 there has been no detectable mutual motion of the pair, hence the orbital period is of about thousands of years (rough estimation from the Kepler's law).

The star is too faint, thus was not observed by Hipparcos satellite, and its distance is therefore rather uncertain. Kharchenko (2001) introduced the parallax 30.29 mas, which is however only an estimate. Its spectral type is also unknown, but the *B–V* index derived from the Tycho catalogue (Høg et al., 2000),  $B–V = 0.89$  mag indicates a spectral type of about K1. On the other hand, the 2MASS infrared photometry (Cutri et al., 2003) gives  $J–H = 0.527$  mag (therefore a spectral type of K3). Finally, Ammons et al. (2006) introduced a temperature corresponding to a spectral type of about K2-3. All these rough spectral estimates were taken from Popper (1980) and Cox (2000).

<sup>★</sup> This paper uses observations made at the South African Astronomical Observatory (SAAO)

<sup>1</sup> <http://ad.usno.navy.mil/wds/>

## 2.2. Light curve

The star was observed by the SuperWASP (Pollacco et al., 2006) project and its complete light curve (hereafter LC) is available. However, we did not use these data for the LC analysis because these were not measured in any standard photometric filter. These data were only used to derive the minima times (see below). We observed the target at the Ondřejov observatory in the Czech Republic with the 65-cm telescope equipped with the CCD camera. For the light curve analysis, only the data from two nights in May 2011 were used (see the electronic data tables). The remaining observations were used for the minima time derivation and to analyze the period changes in the system (see below section 2.3). The observations were obtained in standard *B*, *V*, and *R* filters according to the specification of Bessell (1990).

At first, the complete LC was analyzed using the program PHOEBE (Prša & Zwitter, 2005), which is based on the Wilson-Devinney algorithm (WD, Wilson & Devinney 1971). The derived quantities are as follows: the secondary temperature  $T_2$ , the inclination  $i$ , the luminosities  $L_i$ , the gravity darkening coefficients  $g_i$ , the albedo coefficients  $A_i$ , and the synchronicity parameters  $F_i$ . The limb darkening was approximated using a linear law, and the values of  $x_i$  were interpolated from the van Hamme’s tables, given in van Hamme (1993).

At the beginning of the fitting process, we fixed the temperature of the primary component at  $T_1 = 4700$  K (corresponding to spectral type K3, Cox 2000). In the absence of spectroscopy, the mass ratio was derived via a so-called “q-search method”. This means that we tried different values of mass ratio in the range 1.5 – 0.5 in steps of 0.1 and tried to find the best LC fit according to the lowest value of rms. Finally, we found that the best-fit solution was reached with the value  $q = M_2/M_1 = 0.9$ , which agrees with both eclipses having almost equal depths. For a given mass ratio, the semi-major axis was fixed to an appropriate value for the primary mass to be equal to a typical mass of a particular spectral type (e.g. Popper 1980, Harmanec 1988, or Andersen 1991). With this approach, we were able to estimate the masses, in addition to the radii of both components in absolute units.

However, during the LC fitting process we found that the LC of GK Boo is asymmetric. In particular, the part of the LC near the secondary minimum is distorted in all *BVR* filters. The brightness just after the ascent from the secondary minimum (near the phase 0.6) is higher than the brightness just before the descent (phase 0.4). The difference is about 0.022 mag in *B*, 0.018 mag in *V*, and 0.017 mag in *R* filter, respectively.

With the PHOEBE code, we tried to fix the values of  $A_i$  and  $g_i$  to their appropriate values of 0.5 and 0.32, respectively. However, after then we also allowed these parameters to be fitted, because the fit is tighter (rms). However, probably owing to the asymmetry of the LC these quantities converged to the rather improbable values given in Table 1, and the shape of the observed LC could not be fitted properly. For the asymmetry of the curve, we also tried to introduce a star spot on either of the components. However, no acceptable solution with spot(s) was found to describe the shape of the light curve more accurately in the PHOEBE program. The parameters of the LC fit are given in Table 1, but these cannot sufficiently describe the shape of the LC.

We therefore tried a different code, called ROCHE, developed by Theo Pribulla (Pribulla, 2004), which is also based on the WD code but has for instance also some other computing methods and different controlling of the calculation process. With this program, we used two star spots and similar input pa-

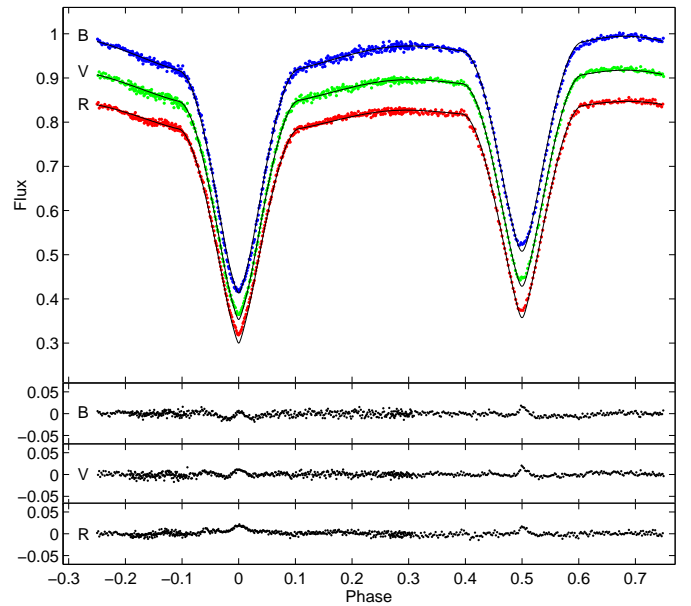


**Fig. 1.** Light curves in *BVR* filters for GK Boo, the solid lines represent the final fit. The residuals after the fit are plotted below. The curves are shifted along y-axis for reasons of clarity.

rameters as described above. At the beginning, the values of  $A_i$  and  $g_i$  were fixed to the appropriate values of 0.5 and 0.32, respectively. However, to achieve a tighter fit both  $A_i$  and  $g_i$  values were also varied across the range from 0 to 1 in steps of 0.05 for both components. The synchronicity parameters  $F_i$  converged to much more reliable values. The value of mass ratio was fixed to  $q = 1.0$  and then also fitted as a free parameter. This was possible because there is a clear distortion of the LC outside the minima (see e.g. Terrell & Wilson 2005). For the fitting process, the two different limb darkening laws were also tried, namely a linear and logarithmic. The latter one provides a much tighter fit to our data. All of the resulting LC parameters are also given in Table 1 (together with parameters of two cooler spots located on the primary component – longitude, latitude, radius and temperature factor). As one can see, the two solutions clearly differ even outside their respective error bars for some of the parameters.

The individual errors in the parameters were not taken from the WD code, but derived in the following way. We computed a range of solutions for GK Boo, which were then used for its error estimation. All solutions with  $\chi^2$  value close to the minimal one (5% from our final solution) were taken and the resultant values of parameters were used to compute the differences between the parameters. The errors in the individual parameters were then computed as a maximum difference and their individual WD errors, given by  $\max(a_i - a_{min}) + \delta a_i + \delta a_{min}$ .

This solution obtained with the ROCHE program provides a much closer fit to the observed data and is the fit plotted in Fig. 1. The value of the eccentricity was fixed at 0 (for a discussion about possible eccentricity see below). Our resultant parameters indicate that both the components are still located on the main sequence, (as required because the age of the Universe does not allow low-mass stars to have evolved from the main sequence). If we follow the assumption of a K3V primary, then the secondary is also of K3V spectral type. These are consistent with the photometric indices presented above, as well as with the individual masses and radii for these types of stars (e.g. Harmanec 1988). An undetectable value of the third light was also resulted derived by this analysis. The presence of photospheric spots on

**Table 1.** Light curve parameters of GK Boo.

Parameter	Value	
	PHOEBE	ROCHE
$T_1$ [K]	4700*	
$T_2$ [K]	$4540 \pm 50$	$4615 \pm 63$
$q (= M_2/M_1)$	$0.9 \pm 0.1$	$0.95 \pm 0.12$
$e$	0*	
$i$ [deg]	$89.83 \pm 0.57$	$89.28 \pm 0.37$
$g_1$	$0.00 \pm 0.04$	$0.35 \pm 0.05$
$g_2$	$0.00 \pm 0.03$	$0.35 \pm 0.05$
$A_1$	$0.00 \pm 0.08$	$0.80 \pm 0.05$
$A_2$	$1.00 \pm 0.08$	$0.80 \pm 0.05$
$F_1$	$1.892 \pm 0.107$	$1.131 \pm 0.096$
$F_2$	$1.866 \pm 0.116$	$1.295 \pm 0.108$
$L_1$ (B) [%]	$54.8 \pm 1.9$	$52.4 \pm 1.1$
$L_2$ (B) [%]	$45.2 \pm 1.8$	$47.6 \pm 1.0$
$L_1$ (V) [%]	$53.5 \pm 1.5$	$51.6 \pm 1.2$
$L_2$ (V) [%]	$46.5 \pm 1.3$	$48.4 \pm 1.1$
$L_1$ (R) [%]	$52.1 \pm 1.4$	$51.1 \pm 1.1$
$L_2$ (R) [%]	$47.9 \pm 1.3$	$48.9 \pm 1.0$
Spots:		
$l_1$ [deg]	–	$287.2 \pm 7.9$
$b_1$ [deg]	–	$60.5 \pm 3.2$
$r_1$ [deg]	–	$37.9 \pm 2.0$
$k_1$	–	$0.75 \pm 0.04$
$l_2$ [deg]	–	$63.3 \pm 7.4$
$b_2$ [deg]	–	$47.4 \pm 12.8$
$r_2$ [deg]	–	$28.7 \pm 4.1$
$k_2$	–	$0.76 \pm 0.04$
Derived quantities:		
$R_1$ [ $R_\odot$ ]	$0.83 \pm 0.18$	$0.89 \pm 0.15$
$R_2$ [ $R_\odot$ ]	$0.86 \pm 0.18$	$0.86 \pm 0.14$
$M_1$ [ $M_\odot$ ]	$0.73 \pm 0.06$	$0.73 \pm 0.06$
$M_1$ [ $M_\odot$ ]	$0.66 \pm 0.06$	$0.70 \pm 0.06$

Note: \* - fixed.

both components of such a late spectral type star is also foreseeable.

### 2.3. Period analysis

To monitor the detailed long-term evolution of the system or its short-period modulation, we collected all available published minima observations. Photometry from the SWASP (Pollacco et al., 2006), ASAS (Pojmanski, 2002), and PiOfTheSky (Burd et al., 2005) projects were used to derive many new minima times for GK Boo. All of these data are given in Table 10, which is available in electronic form only. The method of Kwee & van Woerden (1956) was used. Some of the data were of poor quality, but most were accurate enough to perform a detailed period analysis of the system. The range of these data is about 12 years.

We used these data to analyze the period modulation and found some interesting results. Applying the hypothesis of a third body in the system (the so-called Light-Time Effect, hereafter LITE, described e.g. by Irwin 1959), we found a weak period modulation with a period of about four years. The final fit to the data together with the theoretical curve is shown in Fig. 2. As one can see, there is also some long-term period evolution of the orbital period (the blue dashed line), which was described as a quadratic term in ephemerides. It can be understood as a slow period decrease caused by the mass loss from the system or mass flow between the components (or even momentum loss, magnetic breaking, etc.). Another explanation is that this is only

**Table 2.** Final parameters of the long orbit for GK Boo.

Parameter	Value
	$HJD_0$
$P$ [day]	$0.47777174 \pm 0.00000022$
$p_3$ [day]	$1472.7 \pm 170.0$
$p_3$ [yr]	$4.032 \pm 0.450$
$A$ [day]	$0.0126 \pm 0.0012$
$T_0$	$2454263.3 \pm 1108.3$
$\omega_3$ [deg]	$56.54 \pm 15.0$
$e_3$	$0.084 \pm 0.267$
$Q$ [ $\cdot 10^{-10}$ ]	$-1.071 \pm 0.206$
$f(M_3)$ [ $M_\odot$ ]	$0.000633 \pm 0.000002$
$M_{3,min}$ [ $M_\odot$ ]	$0.115 \pm 0.001$
$M_{3,60}$ [ $M_\odot$ ]	$0.134 \pm 0.002$
$M_{3,30}$ [ $M_\odot$ ]	$0.242 \pm 0.005$
$a_{12} \sin i$ [AU]	$0.217 \pm 0.108$
$a_3$ [mas]	$88.7 \pm 9.8$

part of the long-term period modulation, although we have only limited data coverage.

A more interesting finding is that of a period of about 4 years. Applying the LITE hypothesis, we obtained a final set of parameters given in Table 2, namely the period of the third body  $p_3$ , the semi-amplitude of the effect  $A$ , the time of periastron passage  $T_0$ , the argument of periastron  $\omega_3$ , and the eccentricity  $e_3$ . Despite the low amplitude (about only 1.8 minutes) of the LITE, most of the observed minima times are of higher precision and the modulation is clearly visible. Table 2 also provides the mass function of the third body  $f(M_3)$ , which helps us to estimate its predicted mass.

Having no information about the inclination between the orbits of the eclipsing pair and the hypothetical third body, we plotted Fig. 3, where a plot mass versus inclination is shown. Assuming the coplanar orbits (i.e.  $i_3 = 90^\circ \rightarrow M_3 = M_{3,min}$ ), the resulted minimum mass of the third body is only about  $0.116 M_\odot$ , which places this body at the lower end of stellar masses, hence we can rule out the hypothesis of a brown dwarf or even an exoplanet. Despite of there being no upper limit to this mass (it goes to infinity with  $i_3 \rightarrow 0^\circ$ ), we can estimate a lower limit to the mass. Taking into account that no third light is detected in the LC solution, e.g.  $L_3/(L_1 + L_2) < 0.01$  and assuming a main-sequence star, we can estimate its mass to be lower than  $0.22 M_\odot$ , which is shown in Fig. 3 as a gray area. Further observations are still needed to confirm this hypothesis with higher conclusiveness.

If we assume the parallax of GK Boo as given by Kharchenko (2001),  $\pi = 30.29$  mas, we are also able to compute the angular distance of a hypothetical body to be about 89 mas. This separation of components is well above the limit for modern stellar interferometers. However, there is a problem with the brightness of the third component, which was found to be about more than five magnitudes fainter than the eclipsing pair itself. With the brightness of about 11 mag for the system, this makes a detection impossible. The magnitude difference of the third body with respect to the close pair also clarify why no third light was detected in the LC solution.

Another interesting result was a detection of displaced secondaries. This can be clearly seen in more precise data points (SWASP and our new observations). That secondary minima occur at a different phase of  $\phi_2 \neq 0.5$  from the primary usually indicates that the system is on an eccentric orbit. GK Boo is a well-detached system, so the eccentric orbit cannot be ruled-out easily. Therefore, we assumed an apsidal motion hypothesis for

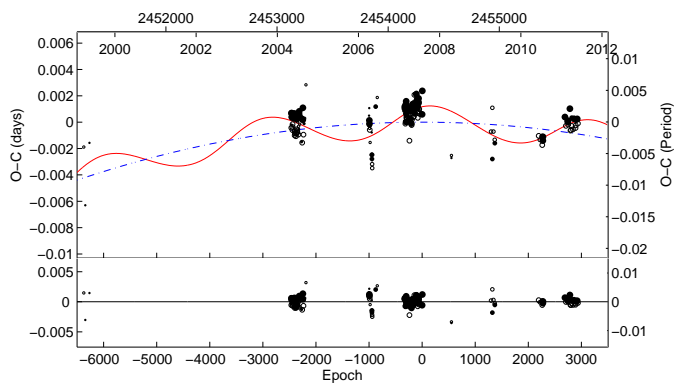


**Fig. 2.** Periodic modulation of period GK Boo. Blue dashed line represents quadratic ephemeris, while red solid line stands for the LITE hypothesis. Residuals are plotted in the bottom plot. The larger the symbol, the higher the weight (higher the precision).

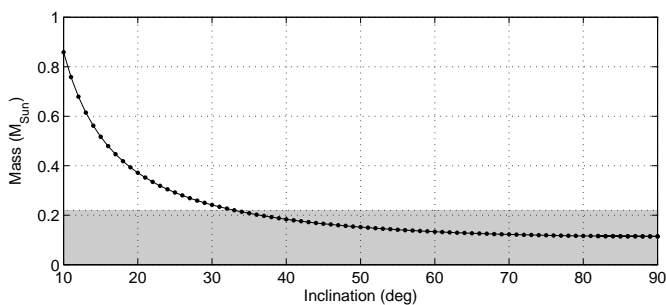


**Fig. 3.** GK Boo: Mass of the third body based on from the LITE hypothesis with respect to the inclination between the orbits.

**Table 3.** Apsidal motion parameters for GK Boo.

Parameter	Value
$e$	$0.0944 \pm 0.0068$
$\omega$ [deg]	$268.9 \pm 2.5$
$\dot{\omega}$ [deg/cycle]	$0.00026 \pm 0.00001$
$U$ [yr]	$1790 \pm 50$

our data set of minima times. We followed a procedure described by e.g. Giménez & García-Pelayo (1983) or Giménez & Bastero (1995) and obtained a set of apsidal motion parameters. The plot of residuals (after subtraction of the LITE fit) with the apsidal motion fit is shown in Fig. 4. It is obviously very slow because the position of secondaries versus primaries changes only very slowly. The resultant values of apsidal motion parameters are given in Table 3.

However, we have to rule out this hypothesis because it lead to unacceptable results. With some information about the physical parameters of both components, we can use the apsidal motion parameters to estimate the internal structure constant. The theoretical  $\log k_{2,theor}$  value taken from Claret (2004) should range from  $-1.35$  to  $-1.65$ . However, the mean value of  $\log k_2$  of both components that can be derived from our solution is very different, even when  $k_2 < 0$ , which is unacceptable. Thus, the system is very probably on a circular orbit.

We may ask why the secondary minima deviate from the 0.5 phase. We published a finding that the displaced secondary minima can also be present in contact binaries where no eccentric orbit is possible (Zasche, 2011), so one cannot perform an ap-

**Table 4.** Methods of minima fitting for GK Boo.

Method of minima fitting	rms	BIC
Linear ephemeris:	0.00151	23.5
Quadratic ephemeris:	0.00119	29.2
LITE and linear ephemeris:	0.00080	51.0
LITE and quadratic ephemeris:	0.00074	56.4
LITE, quadratic ephemeris and apsidal motion:	0.00060	72.6

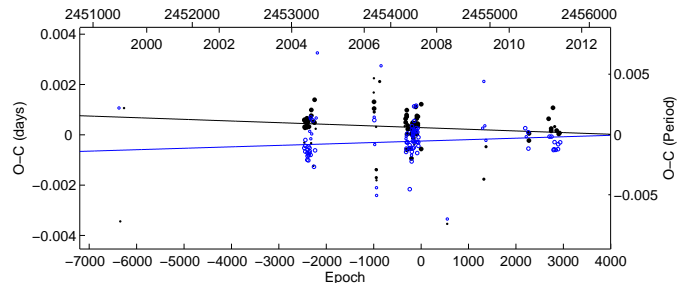


**Fig. 4.**  $O - C$  diagram of GK Boo with the apsidal motion hypothesis, black color is for primary minima, while blue one for secondary.

sidal motion analysis based only on the minima times of a particular system. Some studies found that the secondary minimum is displaced because of the distortion of the LC, thus any standard routine for deriving the time of minimum (e.g. Kwee-van Woerden, bisector chord method or polynomial fitting) cannot be used properly because these consider symmetric minima only. When using these methods to determine minima where both ascending and descending branches have different slopes, we recover only a "false eccentricity".

One can also ask about a significance of the fits presented in Figs. 2 and 4. For this comparison, we summarized different approaches in Table 4. In addition to the rms values, we also provide the values of BIC (Bayesian Information Criterion, see e.g. Liddle 2007), which show the significance of the fit. According to this method, the smaller the rms value, the tighter the fit. To conclude, our final fit provides the smallest rms, but its significance is low and still highly speculative. This is also caused by the poor data coverage, and large scatter in the minima and their low accuracy. Determinations of new more precise minima are therefore needed to confirm or exclude this hypothesis.

### 3. AE For

#### 3.1. Introduction

The Algol-type system AE For (= HIP 14568,  $V_{max} = 10.22$  mag) is also a poorly studied binary. Its published spectral types range from K4 to M0, with the most probable one being K7V as derived by (Torres et al., 2006). The system was presented as a wide double with the star HD 19632 based on their similar parallaxes and proper motions (see Poveda et al. 1994).

Neither the light curve nor the radial velocity curve of AE For have been studied. The star was observed by the Hipparcos satellite and a few times also for the minima observations. It was also continuously monitored with automatic photometric systems such as PiOfTheSky and ASAS. However, the quality of these data do not allow us to use them for a LC analysis. The distance to the system was derived from the Hipparcos data to be  $d = 31.5$  pc.

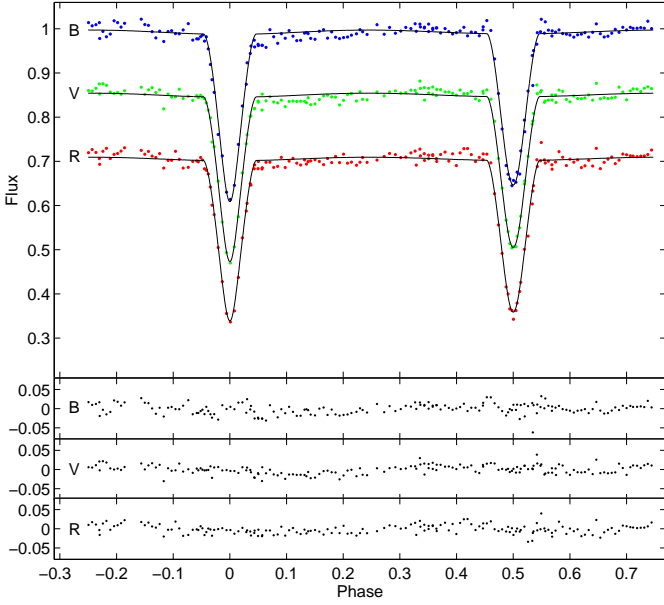


**Fig. 5.** Light curve in *BVR* filters for AE For, the solid line represents the final fit. The curves are shifted along the y-axis for greater clarity.

### 3.2. Light curve

We observed the star from the South African Astronomical Observatory (SAAO) in 2010, using the classical one-channel photoelectric photometer mounted on the 50-cm telescope. All measurements were carefully reduced to the Cousins E-region standard system (Menzies et al., 1989) and corrected for differential extinction.

Thanks to its orbital period close to one day, its complete light curve was observed once in standard *BVR* filters, with some overlapping points (about 170 data points in each filter were obtained). Unfortunately, the quality of the data acquired for several nights was not very good, hence the scatter in the curve is affected by these conditions. Two secondary and one primary minima were observed (see below).

We analyzed our data using the same computational procedure as for GK Boo. The primary temperature was fixed to the appropriate value of 4100 K (sp K7V), the eccentricity was fixed to 0, the values of gravity darkening coefficients were fixed at 0.32, and the albedo coefficients to 0.5 (as recommended for stars with convective envelopes), while the limb darkening coefficients were interpolated from values given in van Hamme (1993). The computational approach was different for the mass ratio  $q$ , which was fixed to  $q = 1.0$  because of the weak outside-eclipse ellipsoidal variations and its detached configuration. In addition, the synchronicity parameters  $F_i$  were set to values of 1.0 for both components. The program ROCHE was used and the resulting LC parameters are given in Table 5, while the final solution is presented in Fig. 5.

One can see that the secondary temperature  $T_2$  is close to the value of  $T_1$ , indicating that the components are similar. Thus, the estimated spectral types of both stars are probably K7V + K7V. Both components are still located on the main sequence and their properties are in agreement with the typical values of K7V stars (as presented by e.g. Harmanec 1988). The third light was also not detected here in any filter. In contrast to GK Boo, the LC of AE For seems to be symmetric.

**Table 5.** Light curve parameters of AE For.

Parameter	Value
$T_1$ [K]	4100*
$T_2$ [K]	4065 ± 48
$q (= M_2/M_1)$	1.0*
$e$	0*
$i$ [deg]	86.51 ± 0.31
$g_1 = g_2$	0.32*
$A_1 = A_2$	0.50*
$F_1 = F_2$	1.000*
$L_1$ (B) [%]	63.2 ± 1.3
$L_2$ (B) [%]	36.8 ± 1.0
$L_1$ (V) [%]	63.1 ± 1.2
$L_2$ (V) [%]	36.9 ± 1.0
$L_1$ (R) [%]	62.6 ± 1.4
$L_2$ (R) [%]	37.4 ± 1.0
Derived quantities:	
$R_1$ [ $R_\odot$ ]	0.66 ± 0.10
$R_2$ [ $R_\odot$ ]	0.52 ± 0.08
$M_1$ [ $M_\odot$ ]	0.50 ± 0.05
$M_2$ [ $M_\odot$ ]	0.50 ± 0.05

Note: \* - fixed.

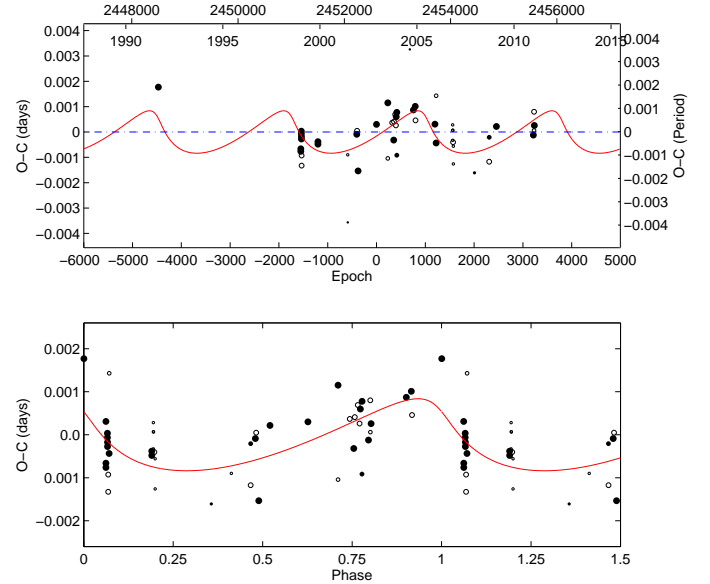


**Fig. 6.** *O* – *C* diagram of AE For. Up: With linear ephemeris. Bottom: With respect to the phase. The data points are fitted with the curve representing the third body hypothesis (see the text for details).

### 3.3. Period analysis

Similarly to GK Boo, we tried to perform the period analysis of all available minima. The collection of minima is much smaller, but thanks to the first observation by Hipparcos (Perryman et al., 1997) these cover a longer time span than for GK Boo. Several new minima were derived based on our new observations from SAAO as well as those from the ASAS and PiOfTheSky surveys.

The same hypothesis as for GK Boo was applied to the data points here. All of the minima times used for the analysis are summarized in Table 11, which is available in electronic form only. As one can see from Fig. 6, there is a clear variation in the minima times. We used the same third-body hypothesis (LITE) as for GK Boo, deriving a final fit to the data given by the parameters in Table 6. The LITE hypothesis resulted in a rather ec-

**Table 6.** Final parameters of the long orbit for AE For.

Parameter	Value
$HJD_0$	$2452605.97070 \pm 0.00035$
$P$ [day]	$0.91820943 \pm 0.00000012$
$p_3$ [day]	$2524.6 \pm 149.6$
$p_3$ [yr]	$6.912 \pm 0.409$
$A$ [day]	$0.00083 \pm 0.00032$
$T_0$	$2453548.8 \pm 413.1$
$\omega_3$ [deg]	$146.2 \pm 57.8$
$e_3$	$0.601 \pm 0.414$
$f(M_3)$ [ $M_\odot$ ]	$0.000098 \pm 0.000001$
$M_{3,min}$ [ $M_\odot$ ]	$0.047 \pm 0.001$
$M_{3,60}$ [ $M_\odot$ ]	$0.055 \pm 0.001$
$M_{3,30}$ [ $M_\odot$ ]	$0.098 \pm 0.003$
$a_{12} \sin i$ [AU]	$0.167 \pm 0.064$
$a_3$ [mas]	$117.2 \pm 8.3$

**Table 7.** Methods of minima fitting for AE For.

Method of minima fitting	rms	BIC
Linear ephemeris:	0.000255	24.4
LITE and linear ephemeris:	0.000163	44.8

centric orbit, although the result is affected by a relatively large error, hence maybe the  $e_3$  value should be lower. Only additional observations would help us confirm or refute this hypothesis, refine the period, and possibly detect some long-term evolution of the period similar to that in GK Boo, because the first observation from Hipparcos deviates significantly from the fit. With the same procedure as for GK Boo, we computed the significance of the fits according to the BIC criterion (see Table 7). As one can see, the fit is still very poor and highly speculative. However, using only the linear ephemeris, there remains a clear quasi-sinusoidal variation, which needs some physical explanation.

From the LITE parameters, we were able to calculate the minimal mass of the third body (i.e. coplanar orbits), which we found to be only about  $47 M_{Jup}$ , which is even lower than the limit of stellar masses. Therefore, if the orbits were coplanar (which only would be our assumption, because the process of tidal coplanarization is very slow), the third body would very probably be a brown dwarf (exoplanets have masses about one half of this value). With such a body, we reach minimal masses that can be detected by this method, because the amplitude of LITE is comparable to the typical precision of individual minima-time measurements. Whatever applies to the possible interferometric detection of GK Boo companion also applies here, because its luminosity is too low.

#### 4. Discussion and conclusions

We have derived preliminary light-curve solutions and period analyses of the poorly studied Algol-type eclipsing binaries GK Boo and AE For, which we have found to have several interesting and similar features. Since both of them are low-mass stars of very similar types (K3+K3 for GK Boo, and K7+K7 for AE For), both of them have short orbital periods. Moreover, both are relatively close to the Sun and also appear to contain third bodies in their systems, which cause a periodic modulation of the orbital periods of both systems. Assuming a coplanar orbit, for AE For this third body appears to be a brown dwarf, which makes this system even more interesting. However, more photo-

metric and spectroscopic observations are needed to confirm or refute this hypothesis.

The system GK Boo has an asymmetric light curve, which is the probably accounts for the shift in the secondary minimum in phase with the primary one. The apsidal motion hypothesis cannot explain this discrepancy.

In general, if the third body hypothesis as proposed based on the period analysis is found to be the correct one, here we have considered quite curious examples of hierarchical quadruple systems of low masses. As far as we know, there are only a few similar multiple late-type systems for which one of the components is an eclipsing binary (e.g. BB Scl or MR Del).

*Acknowledgements.* We thank the "ASAS", "SWASP" and "Pi of the sky" teams for making all of the observations easily public available. PZ wish to thank the staff at SAAO for their warm hospitality and help with the equipment. Authors are also grateful to Theo Pribulla for his helpful comments about the ROCHE code. An anonymous referee is also acknowledged for his/her helpful and critical suggestions. This work was supported by the Czech Science Foundation grant no. P209/10/0715 and also by the Research Programme MSM0021620860 of the Czech Ministry of Education. This research has made use of the SIMBAD database, operated at CDS, Strasbourg, France, and of NASA's Astrophysics Data System Bibliographic Services.

#### References

Ammons, S. M., Robinson, S. E., Strader, J., Laughlin, G., Fischer, D., & Wolf, A. 2006, *ApJ*, 638, 1004  
 Andersen, J. 1991, *A&A Rev.*, 3, 91  
 Bessell, M. S. 1990, *PASP*, 102, 1181  
 Burd, A., et al. 2005, *NewA*, 10, 409  
 Claret, A. 2004, *A&A*, 424, 919  
 Cox, A. N. 2000, *Allen's Astrophysical Quantities*,  
 Cutri, R. M., et al. 2003, *VizieR Online Data Catalog*, 2246, 0  
 Giménez, A., & García-Pelayo, J. M. 1983, *Ap&SS*, 92, 203  
 Giménez, A., & Bastero, M. 1995, *Ap&SS*, 226, 99  
 van Hamme, W. 1993, *AJ*, 106, 2096  
 Harmanec, P. 1988, *BAICz*, 39, 329  
 Høg, E., et al. 2000, *A&A*, 355, L27  
 Irwin, J. B. 1959, *AJ*, 64, 149  
 Kharchenko, N. V. 2001, *Kinematika i Fizika Nebesnykh Tel*, 17, 409  
 Kroupa, P. 2002, *Science*, 295, 82  
 Kwee, K.K., van Woerden, H. 1956, *BAN*, 12, 327  
 Lada, C. J. 2006, *ApJ*, 640, L63  
 Liddle, A. R. 2007, *MNRAS*, 377, L74  
 Mason, B. D., Wycoff, G. L., Hartkopf, W. I., Douglass, G. G., & Worley, C. E. 2001, *AJ*, 122, 3466  
 Menzies, J.W., Cousins, A.W.J., Banfield, R.M., Laing, J.D. 1989, *SAAOC* 13, 1  
 Perryman, M. A. C., Lindegren, L., Kovalevsky, J., et al. 1997, *A&A*, 323, L49  
 Pojmanski, G. 2002, *AcA*, 52, 397  
 Pollacco, D. L., et al. 2006, *PASP*, 118, 1407  
 Popper, D. M. 1980, *ARA&A*, 18, 115  
 Poveda, A., Herrera, M. A., Allen, C., Cordero, G., & Lavalley, C. 1994, *RMxAA*, 28, 43  
 Pribulla, T. 2004, *Spectroscopically and Spatially Resolving the Components of the Close Binary Stars*, 318, 117  
 Prša, A., & Zwitter, T. 2005, *ApJ*, 628, 426  
 Terrell, D., & Wilson, R. E. 2005, *Ap&SS*, 296, 221  
 Torres, C. A. O., Quast, G. R., da Silva, L., de La Reza, R., Melo, C. H. F., & Sterzik, M. 2006, *A&A*, 460, 695  
 Wilson, R. E., & Devinney, E. J. 1971, *ApJ*, 166, 605  
 Zasche, P. 2011, *IBVS*, 5991, 1

**Table 8.** Heliocentric minima of GK Boo used for the analysis. **Table 9.** Minima of GK Boo, cont.

HJD - 2400000	Error	Type	Filter	Reference
51260.8547	0.0007	sec	-	IBVS 5060
51273.9890		prim	-	A.Paschke - Rotse
51311.7377	0.0004	prim	-	IBVS 5060
53128.46588	0.00024	sec	-	SWASP
53128.70498	0.00041	prim	-	SWASP
53129.66141	0.00056	prim	-	SWASP
53130.61697	0.00047	prim	-	SWASP
53132.52777	0.00021	prim	-	SWASP
53135.39435	0.00010	prim	-	SWASP
53137.54360	0.00024	sec	-	SWASP
53138.49891	0.00028	sec	-	SWASP
53139.45491	0.00021	sec	-	SWASP
53141.60560	0.00027	prim	-	SWASP
53152.59424	0.00025	prim	-	SWASP
53153.54982	0.00020	prim	-	SWASP
53154.50553	0.00017	prim	-	SWASP
53155.46071	0.00015	prim	-	SWASP
53156.41642	0.00014	prim	-	SWASP
53158.56492	0.00048	sec	-	SWASP
53159.52074	0.00022	sec	-	SWASP
53160.47640	0.00021	sec	-	SWASP
53161.43169	0.00026	sec	-	SWASP
53163.58313	0.00031	prim	-	SWASP
53164.53862	0.00031	prim	-	SWASP
53165.49392	0.00015	prim	-	SWASP
53166.44965	0.00020	prim	-	SWASP
53169.55361	0.00034	sec	-	SWASP
53170.50939	0.00024	sec	-	SWASP
53171.46489	0.00034	sec	-	SWASP
53172.42077	0.00031	sec	-	SWASP
53175.52707	0.00024	prim	-	SWASP
53176.48289	0.00047	prim	-	SWASP
53180.54262	0.00022	sec	-	SWASP
53181.49835	0.00017	sec	-	SWASP
53182.45376	0.00018	sec	-	SWASP
53183.41009	0.00076	sec	-	SWASP
53191.53267	0.00080	sec	-	SWASP
53192.48678	0.00031	sec	-	SWASP
53193.44381	0.00026	sec	-	SWASP
53194.39850	0.00045	sec	-	SWASP
53197.50383	0.00080	prim	-	SWASP
53198.46046	0.00023	prim	-	SWASP
53199.41623	0.00026	prim	-	SWASP
53203.47632	0.00029	sec	-	SWASP
53209.44918	0.00047	prim	-	SWASP
53215.42110	0.00040	sec	-	SWASP
53220.43588	0.00083	prim	-	SWASP
53221.39317	0.00039	prim	-	SWASP
53226.40796	0.00058	sec	-	SWASP
53231.42630	0.00045	prim	-	SWASP
53232.38275	0.00032	prim	-	SWASP
53237.39732	0.00033	sec	-	SWASP
53243.37030	0.00082	prim	-	SWASP
53248.38731	0.00078	sec	-	SWASP
53259.85637	0.00078	sec	-	SWASP
53827.68574	0.00085	prim	-	SWASP
53829.59740	0.00088	prim	-	SWASP
53830.55201	0.00069	prim	-	SWASP
53831.50729	0.00051	prim	-	SWASP
53832.46270	0.00015	prim	-	SWASP
53832.70138	0.00024	sec	-	SWASP
53833.65681	0.00047	sec	-	SWASP
53837.47803	0.00029	sec	-	SWASP
53851.57305	0.00105	prim	-	SWASP
53852.52690	0.00049	prim	-	SWASP
53853.48213	0.00027	prim	-	SWASP
53854.43799	0.00032	prim	-	SWASP
53855.39312	0.00090	prim	-	SWASP
53855.63171	0.00037	sec	-	SWASP
53856.58695	0.00051	sec	-	SWASP
53887.40789	0.00024	prim	-	SWASP
53901.50285	0.00080	sec	-	SWASP
54140.62657	0.00022	prim	-	SWASP
54149.70458	0.00021	prim	-	SWASP
54150.65998	0.00028	prim	-	SWASP
54153.76487	0.00119	sec	-	SWASP
54154.71989	0.00026	sec	-	SWASP
54155.67581	0.00061	sec	-	SWASP
54156.63161	0.00053	sec	-	SWASP
54157.58667	0.00065	sec	-	SWASP
54159.73799	0.00019	prim	-	SWASP
54160.69347	0.00018	prim	-	SWASP
54161.64928	0.00022	prim	-	SWASP
54162.60325	0.00019	prim	-	SWASP

HJD - 2400000	Error	Type	Filter	Reference
54163.55942	0.00065	prim	-	SWASP
54165.70909	0.00037	sec	-	SWASP
54166.66462	0.00022	sec	-	SWASP
54167.62053	0.00034	sec	-	SWASP
54170.72638	0.00023	prim	-	SWASP
54171.68178	0.00043	prim	-	SWASP
54189.59755	0.00032	sec	-	SWASP
54190.55322	0.00019	sec	-	SWASP
54191.50702	0.00053	sec	-	SWASP
54194.61418	0.00029	prim	-	SWASP
54195.57050	0.00029	prim	-	SWASP
54202.49743	0.00046	sec	-	SWASP
54206.55909	0.00039	prim	-	SWASP
54208.46922	0.00027	prim	-	SWASP
54208.70823	0.00143	sec	-	SWASP
54210.61908	0.00030	sec	-	SWASP
54212.53056	0.00050	sec	-	SWASP
54213.48698	0.00049	sec	-	SWASP
54214.44267	0.00029	sec	-	SWASP
54214.68147	0.00039	prim	-	SWASP
54215.63620	0.00057	prim	-	SWASP
54216.59233	0.00019	prim	-	SWASP
54217.54805	0.00038	prim	-	SWASP
54218.50359	0.00021	prim	-	SWASP
54219.45928	0.00030	prim	-	SWASP
54220.41494	0.00069	prim	BVR	PS
54220.41498	0.00029	prim	-	SWASP
54222.56423	0.00066	sec	BVR	PS
54222.56444	0.00028	sec	-	SWASP
54223.51949	0.00169	sec	BVR	PS
54223.51994	0.00108	sec	-	SWASP
54224.47565	0.00035	sec	-	SWASP
54225.43110	0.00022	sec	-	SWASP
54225.67010	0.00026	prim	-	SWASP
54226.38671	0.00034	sec	-	SWASP
54226.62544	0.00036	prim	-	SWASP
54227.58111	0.00026	prim	-	SWASP
54228.53676	0.00031	prim	-	SWASP
54230.44800	0.00019	prim	-	SWASP
54231.40365	0.00019	prim	-	SWASP
54231.64168	0.00048	sec	-	SWASP
54232.59790	0.00032	sec	-	SWASP
54233.55304	0.00025	sec	-	SWASP
54234.50899	0.00034	sec	-	SWASP
54235.46550	0.00054	sec	-	SWASP
54236.42047	0.00028	sec	-	SWASP
54236.65842	0.00085	prim	-	SWASP
54237.37517	0.00137	sec	BVR	PS
54239.52553	0.00091	prim	BVR	PS
54249.55879	0.00027	prim	-	SWASP
54250.51471	0.00031	prim	-	SWASP
54251.47023	0.00057	prim	-	SWASP
54252.42644	0.00028	prim	-	SWASP
54254.57647	0.00059	sec	-	SWASP
54256.48657	0.00172	sec	BVR	PS
54256.48655	0.00039	sec	-	SWASP
54257.44222	0.00025	sec	-	SWASP
54261.50367	0.00031	prim	-	SWASP
54262.45860	0.00020	prim	-	SWASP
54263.41487	0.00037	prim	-	SWASP
54265.56380	0.00079	sec	-	SWASP
54266.51892	0.00042	sec	-	SWASP
54267.47491	0.00020	sec	-	SWASP
54268.43084	0.00017	sec	-	SWASP
54271.53663	0.00070	prim	-	SWASP
54272.49225	0.00033	prim	-	SWASP
54273.44808	0.00026	prim	-	SWASP
54276.55314	0.00095	sec	-	SWASP
54277.50813	0.00065	sec	-	SWASP
54278.46353	0.00031	sec	-	SWASP
54279.41942	0.00021	sec	-	SWASP
54305.45758	0.00157	prim	BVR	PS
54307.37045	0.00141	prim	BVR	PS
54568.70649	0.00072	prim	-	Piofthesky
54568.94557	0.00097	sec	-	Piofthesky
54925.36514	0.0001	sec	R	OEJV 107
54937.3112	0.0020	sec	Ir	IBVS 5918
54937.5462	0.0005	prim	Ir	IBVS 5918
54947.34260	0.0014	sec	R	OEJV 107
54958.8085	0.0007	sec	V	IBVS 5894
54959.52489	0.0001	prim	R	OEJV 107
55354.40380	0.00148	sec	BVR	PS
55364.4367	0.0001	sec	BVRI	IBVS 5965
55385.45891	0.00131	sec	BVR	PS

**Table 10.** Minima of GK Boo, cont.

HJD - 2400000	Error	Type	Filter	Reference
55386.41381	0.00104	sec	BVR	PS
55391.43075	0.00097	prim	BVR	PS
55392.38658	0.00113	prim	BVR	PS
55590.66335	0.00036	prim	-	RU
55599.50146	0.00018	sec	-	RU
55616.46275	0.00005	prim	B	PZ
55616.46266	0.00012	prim	R	RU
55619.56796	0.00010	sec	R	RU
55634.61898	0.00016	prim	R	RU
55640.58947	0.00019	sec	R	RU
55644.41169	0.00005	sec	B	PZ
55650.62303	0.00014	sec	R	RU
55651.34031	0.00113	prim	B	PZ
55662.56706	0.00013	sec	R	RU
55671.40664	0.00007	prim	VR	PZ
55685.50021	0.00012	sec	R	RU
55687.41150	0.00011	sec	BVR	PZ
55692.42853	0.00004	prim	BVR	PZ
55700.55071	0.00004	prim	BVR	PZ
55707.47805	0.00008	sec	BVR	PZ

**Table 11.** Heliocentric minima of AE For used for the analysis.

HJD - 2400000	Error	Type	Filter	Reference
48500.6581	0.001	prim	Hp	Hipparcos
51180.9089		prim	R	VSOLJ 37
51180.9090	0.0002	prim	R	VSOLJ 47
51191.0099		prim	R	VSOLJ 37
51191.0100	0.0002	prim	R	VSOLJ 47
51191.9279		prim	V	VSOLJ 37
51191.9280	0.0001	prim	V	VSOLJ 47
51196.9770	0.0001	sec	R	VSOLJ 47
51196.9774		sec	R	VSOLJ 37
51504.11886		prim	I	VSOLJ 37
51504.1190	0.0002	prim	I	VSOLJ 47
52065.14178	0.00121	prim	V	ASAS
52065.60355	0.0025	sec	V	ASAS
52235.0140		prim	I	VSOLJ 39
52240.9825		sec	I	VSOLJ 39
52258.8860	0.0002	prim	R	VSOLJ 39
52605.9710		prim	I	VSOLJ 40
52818.07823	0.00077	prim	V	ASAS
52818.53514	0.00165	sec	V	ASAS
52901.1754		sec	I	VSOLJ 42
52929.1801		prim	I	VSOLJ 42
52936.0674		sec	I	VSOLJ 42
52957.1865		sec	V	VSOLJ 42
52970.0410		sec	I	VSOLJ 42
52976.0097		prim	I	VSOLJ 42
52987.0267		prim	V	VSOLJ 42
52987.9466		prim	I	VSOLJ 42
53300.1379		prim	V	VSOLJ 43
53335.0300		prim	V	VSOLJ 43
53340.0796		sec	V	VSOLJ 43
53705.0677	0.0002	prim	V	VSOLJ 44
53728.02219	0.00093	prim	V	ASAS
53728.48316	0.00194	sec	V	ASAS
54039.75501	0.00027	sec	-	PiOfTheSky
54040.67301	0.00045	sec	-	PiOfTheSky
54047.1000	0.0001	sec	V	VSOLJ 45
54052.60840	0.00149	sec	-	PiOfTheSky
54448.81542	0.00039	prim	-	PiOfTheSky
54726.11607	0.00187	prim	V	ASAS
54726.57421	0.00131	sec	V	ASAS
54862.9297	0.0002	prim	V	VSOLJ 50
55558.0139		prim	V	VSOLJ 51
55570.41065	0.00072	sec	BVR	PZ - SAAO
55571.32812	0.00105	sec	BVR	PZ - SAAO
55576.37847	0.00065	prim	BVR	PZ - SAAO